

H.E. Mindak

Fig. 1. Map of the bay area: general areas of thermal cracking are represented by heavy black lines, contours show trends of ice thickness in centimetres on January 30, 1956, inset gives general location of Hopedale.

OBSERVATIONS ON THE PHYSICAL PROPERTIES OF SEA-ICE AT HOPEDALE, LABRADOR*†

Wilford F. Weeks** and Owen S. Lee††

Introduction

DURING the winter in the northern hemisphere alone over 16 million square kilometres of ocean surface are covered by ice. This is roughly an area twice the size of the United States or eight times the area covered by glaciers. Some efforts have been made to interpret drift patterns of sea-ice and their effect on the movement of ships and to develop methods of forecasting sea-ice formation and growth from known meteorological parameters. However, very little is known concerning the detailed behaviour and growth of this material (Armstrong, 1956).

During the last three winters the Air Force Cambridge Research Center, the Navy Hydrographic Office and the Snow, Ice, and Permafrost Research Establishment have sponsored a joint project to study the general physical properties of sea-ice by direct observations in the field. This paper reports some preliminary results obtained from data collected during the winter of 1955 to 1956 at Hopedale, Labrador.

Physical setting

Hopedale is a village on the Labrador coast approximately 125 miles north of Goose Bay. This location offers an opportunity to study the formation of sea-ice in a protected bay, which has a typical subarctic climate. The general configuration of the bay is shown in Fig. 1. It is protected from heavy wave action by a number of small islands that extend as far as 10 miles from the coast-line. The tides in the harbour are semi-diurnal and are approximately 2 metres in height. There are no appreciable currents in the harbour and, with one exception, no thin areas were noticed in the ice cover due to the action of tidal currents.

* The statements in this paper represent the opinion of the authors and are not to be construed as an official release from the U.S. Navy Electronics Laboratory or the U.S. Navy Hydrographic Office.

† A portion of this paper was read at the Washington, D.C. meeting of the American Geophysical Union, May 2, 1957 (Weeks and Lee, 1957).

** Department of Geology, Washington University, St. Louis 5, Missouri, U.S.A.

†† U.S. Navy Electronics Laboratory, Physical Oceanography Section, San Diego 52, California, U.S.A.

The water of the bay, as any sea-water with a salinity greater than 24.7‰, has a freezing point higher than the temperature of maximum density. Surface cooling creates an unstable vertical density distribution, which causes convective mixing. This process transports the sensible heat, which is stored in the lower layers of the water, to the surface where it is dissipated. At the time of initial ice-formation the bay water is practically free of sensible heat and it remains isothermal at the freezing point during the winter. A relatively small amount of sensible heat becomes available as freezing releases salts to the underlying water and lowers the freezing point. The average salinity during the period of freezing is 32.7‰ and the average freezing point is -1.8°C .

Formation of the initial ice-cover

Initial ice-formation took place during slight to medium wave action. First small plate-like dendrites of pure ice were noted in the upper 10 cm. of the water near shore. These crystals were extremely fragile and variable in lateral dimensions. They were 0.5 cm. to 2.5 cm. wide and had a squarish or irregular outline. Their height varied from 0.1 mm. to 1 mm.

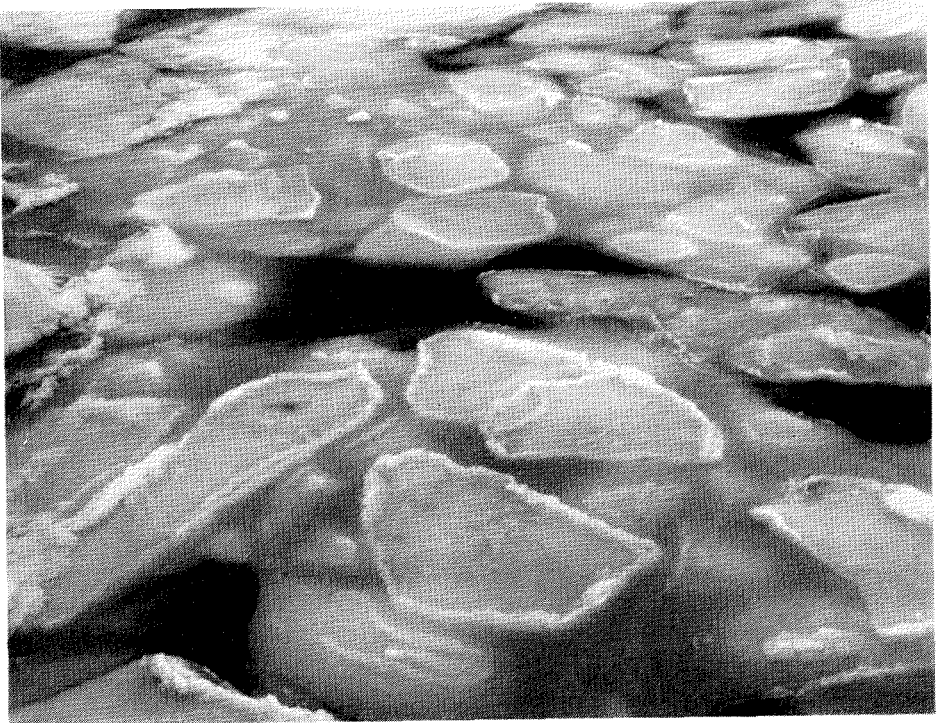


Fig. 2. Unconsolidated pancakes separated by frazil slush and clear water (the dark areas).



Fig. 3. Pancakes undergoing abrasion due to heavy wave motion.

The movement of the water caused these crystals to brush against each other and to disintegrate until a "mush" of crystal fragments formed. As freezing continued, this "mush" layer began to congeal into pancake-like bodies (Fig. 2), which continually changed in shape owing to abrasion from surrounding pancakes and slight wave motion. (Fig. 3). The diameters of the pancakes varied from 0.2 m. to 4.0 m. The appearance of the closely compacted pancakes was similar to a giant jigsaw puzzle. The general shape of the pancakes depended on their position with respect to wave motion and the shore. In the open ocean, where no fixed boundaries were present, the pancakes were usually circular in outline owing to constant abrasion by other pancakes, which tended to remove sharp corners. Close to shore the motion came from only one direction (the direction of open water) and the pancakes were commonly non-equidimensional with their long axes parallel to the shore-line. Fig. 4 shows a newly formed ice-sheet composed entirely of small pancakes cemented together by a mush of frazil-crystals.

During calm periods, usually at night, sheet-ice formed. Sheet-ice on a lake has been described by Wilson, Zumberge, and Marshall (1954) as "an ice-cover which presents a smooth unbroken surface on which there are no highly evident horizontal changes in the structure of the ice layer".



Fig. 4. Newly formed ice-sheet composed entirely of small pancakes cemented together by a mush of frazil crystals.

This definition is also applicable to sea-ice. Where surface waves are present the ice-cover that forms has an initial thickness of 8 cm. to 10 cm. In contrast, sheet-ice has an initial thickness of the order of a few millimetres. It usually starts to form at foreign objects or at the edge of an existing ice-sheet. From there it grows outward as a very thin film with a definite advancing front. After large sections of Hopedale Bay were covered with sheet-ice it also formed in holes where freezing was delayed and in areas where ice blocks had been removed for study (Fig. 5). After the initial ice-sheet had formed, sheet-ice developed beneath joined pancakes and slush-ice to form a composite ice-sheet (Fig. 6).

Sheet-ice is composed of vertically elongated crystals, which extend from a few millimetres below the top of the ice to the bottom. The crystal diameters vary from a fraction of a millimetre to 20 cm. The brine pockets and air bubbles occur in a series of parallel layers in the ice crystals. The average distance between the midpoints of two successive brine layers is approximately 0.45 mm. Sea-ice crystals below the upper 5 cm. of the ice-sheet are characterized by *c*-axes (Fig. 7) that always lie parallel to the water-surface. In marked contrast both vertical and horizontal *c*-axis orientations were observed in lake-ice at Hopedale (Fig. 8). Pronounced vertical *c*-axis orientations have commonly been observed in lake-ice (Wilson, Zum-berge and Marshall, 1954). However, recent unpublished data indicate that

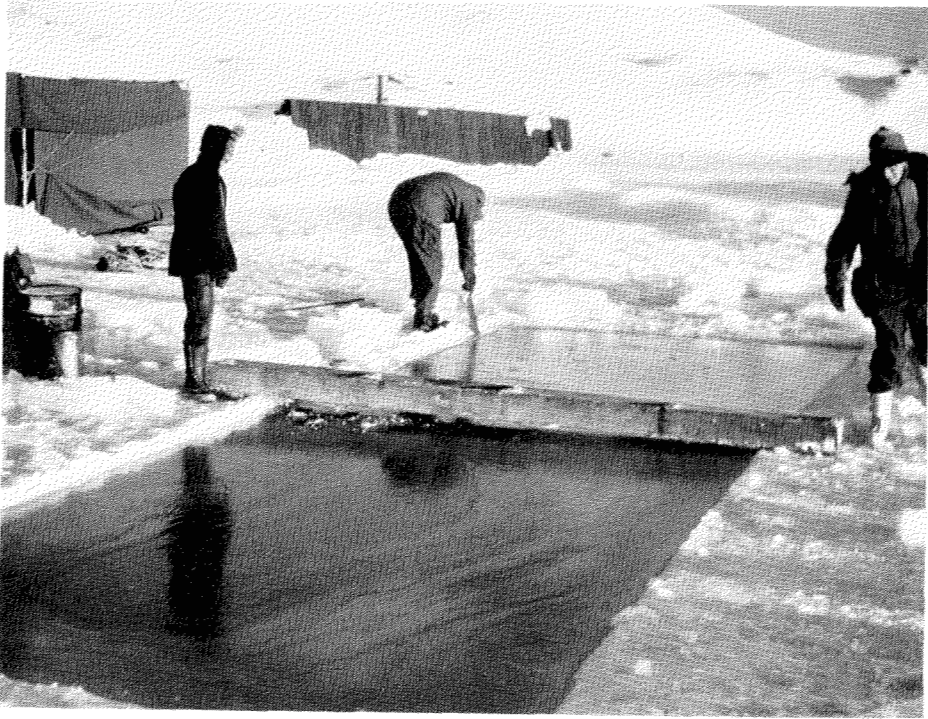


Fig. 5. Rectangular test pond cut in the ice-sheet that has frozen over with sheet-ice.

the horizontal *c*-axis orientations observed at the Hopedale lake are not uncommon (E. W. Marshall, personal communication).

A large number of thin sections and crystal impressions of sea-ice were made at Hopedale to determine (a) the distribution of brine and the method of its movement through the ice-sheet and (b) the reasons for the pronounced horizontal *c*-axis orientation. The results of this crystallographic study will be published later (Weeks, 1958).

Salinity of the initial ice-cover

The salinities presented here were determined by hydrometers that were calibrated directly in salinity. The samples were collected by drilling vertically into the ice with a 7.6-cm.-diameter ice-corer (Bader, 1957). The core was immediately cut into 7.6-cm. segments (3-cm segments for thin ice), placed in sealed containers, melted, and brought to a temperature of approximately 15°C. The water temperature and salinity were then measured and suitable temperature corrections were applied to give the salinity of the water sample at 15°C. Graphs of ice salinity versus depth in the ice-sheet gave curves without sharp discontinuities and irregularities.

Fig. 9 gives profiles of a series of successive salinity samples, which were taken between the dates December 23 and 29, 1955 from thin ice north of

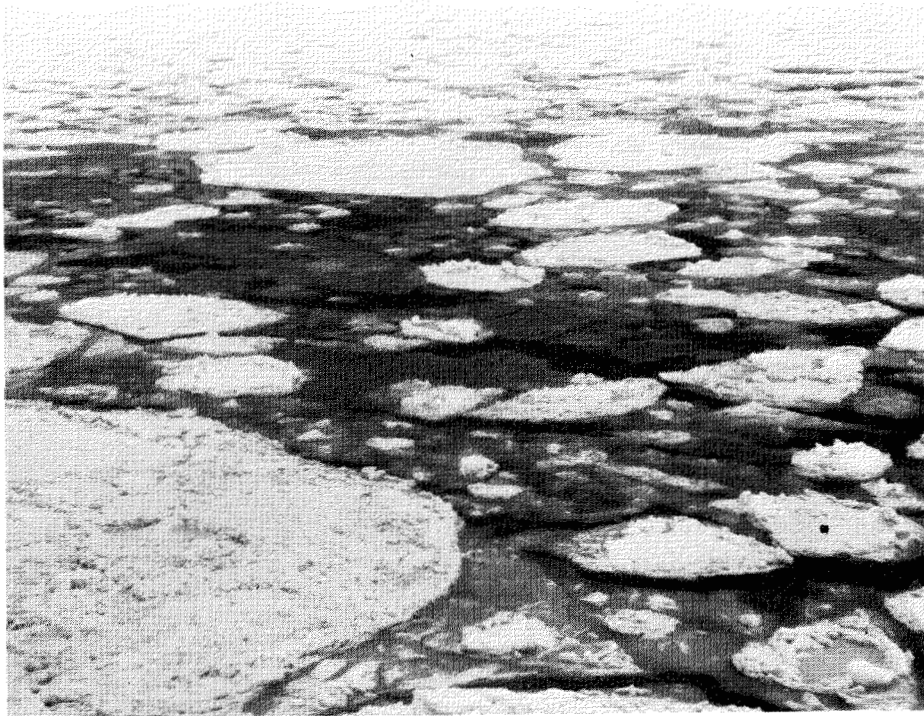


Fig. 6. Composite ice-sheet consisting of old pancakes of varying size, grey areas of frazil slush-ice and black areas of newly formed thin sheet-ice.

Hopedale dock. The uppermost 7.5 cm. of these cores were composed of slush-ice that formed from a mixture of frazil- and snow-crystals. Ice below this layer was normal sheet-ice with the typical vertical crystal structure. Fig. 10 shows successive salinity profiles taken from pure sheet-ice that had formed on a very calm night. These data were collected between December 25, 1955 and January 24, 1956. By comparing Fig. 10 with Fig. 9 the following observations can be made:

1. The salinity of the ice-sheet drops off rapidly with time.
2. Initially the surface layer of the ice-sheet has a higher brine content than the lower part of the sheet.
3. The crystal structure of an ice-sheet is one of the more important factors that control brine drainage from sea-ice (the slush-ice layer in Fig. 9 has a much higher salinity than the ice of Fig. 10 because brine drains more slowly in the former). This slower brine drainage in slush-ice is attributed to poorer vertical orientation of brine cells.

Formation of infiltrated snow-ice

Between freeze-up and January 6 the air temperature (averaged over 24 hours) remained below -10°C . (Fig. 11) and normal sea-ice growth

resulted. On January 7 the average air temperature rose to -6°C . and a storm began with high winds and heavy snow (up to 30 cm.). When the storm subsided a thin layer of brine-saturated slush began to form at the base of the snow layer. The weight of the fallen snow had depressed the surface of the ice-sheet below the water-level. Brine present in the sea-ice was displaced by water from below and moved into the overlying snow until hydrostatic equilibrium was attained. This process formed a briny slush layer between the surface of the sea-ice and the overlying dry snow layer. The thickness of this slush layer increased as the warm period continued and the brine migrated through the ice until the slush layer reached a maximum thickness of 11.5 cm. In places the complete snow layer was converted to slush.

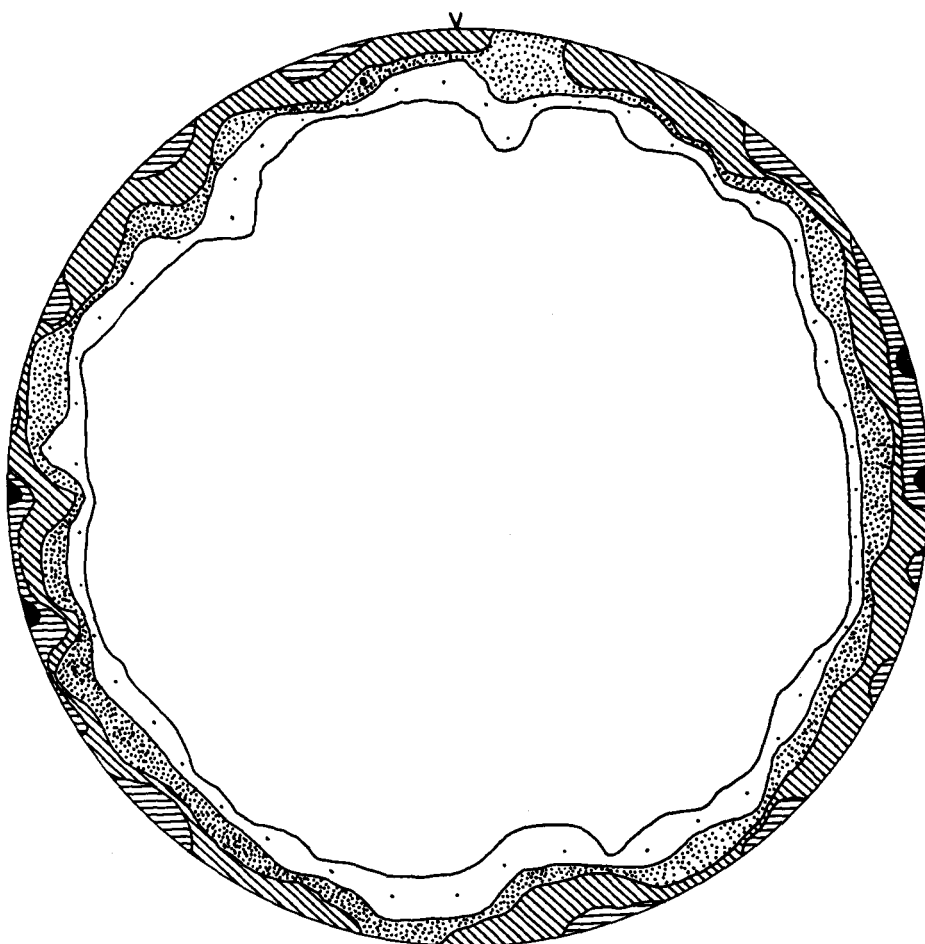


Fig. 7. Orientation of sea-ice c-axes plotted on the upper hemisphere of a Schmidt net. Diagram is in the horizontal plane, 200 grains, contours represent 1, 2, 4, 6, and 9 per cent per 1 per cent area.

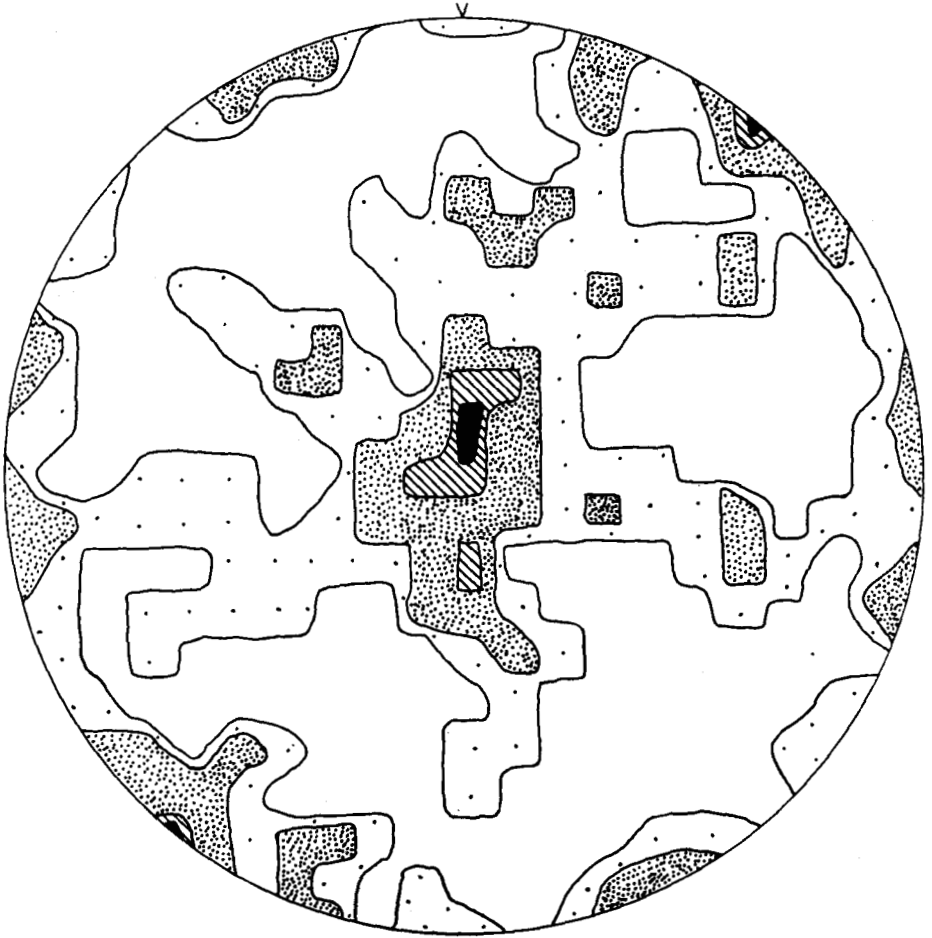


Fig. 8. Orientation of lake-ice c-axes plotted on the upper hemisphere of a Schmidt net. Diagram is in the horizontal plane, 150 grains, contours represent 1, 2, 4, and 5 per cent per 1 per cent area.

Accelerated formation of slush occurred near open tidal and thermal cracks. Early in the slush-forming process holes were drilled through the ice and artesian water fountains (up to 9 cm. high) appeared. Thick slush layers immediately formed in the vicinity of each hole. This showed that during the earlier stages of slush-formation, when the upper part of the sea-ice was colder than a certain critical temperature, the ice-sheet was impermeable and the passage of brine into the snow was inhibited. When the ice temperature rose enough for the brine pockets to interconnect and allow passage of brine through the ice-sheet, the slush layer began to form. If the entire slush layer over the whole bay was formed only by the movement of water through cracks, the slush would form quite rapidly in one or two days, instead of forming slowly during a period of weeks.

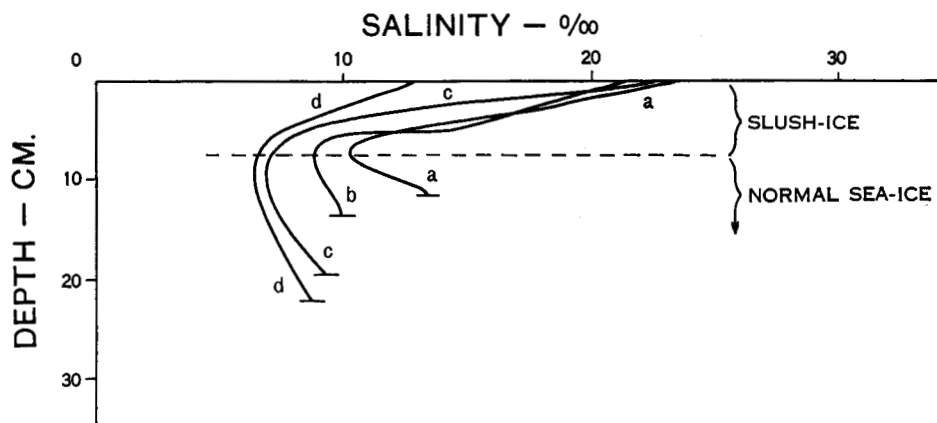


Fig. 9. Salinity profiles from sea-ice that formed during a period of wave action. Dates of profiles are: a December 23, b December 24, c December 26, and d December 29, 1955.

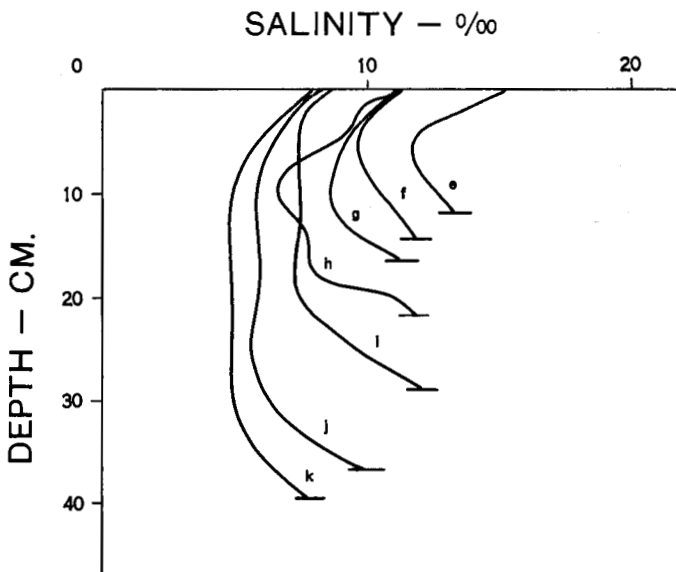


Fig. 10. Salinity profiles from sheet sea-ice. Dates of profiles are: e December 25, f December 26, g December 28, h December 30, 1955; i January 3, j January 14, and k January 24, 1956.

Taking the average salinity of the ice-sheet during the slush-forming period as 6‰ to 8‰ it is possible to estimate roughly this critical ice temperature as *ca.* -3° to -4°C . Below the critical temperature the brine content is uniformly low, whereas above the critical temperature the volume of brine increases rapidly with increasing temperature (Anderson and Weeks, 1958, Fig. 5). Most of the upward migration of brine probably occurs during the daylight hours of cloud-free days when the ice is frequently warmed to the critical temperature by absorption of radiation.

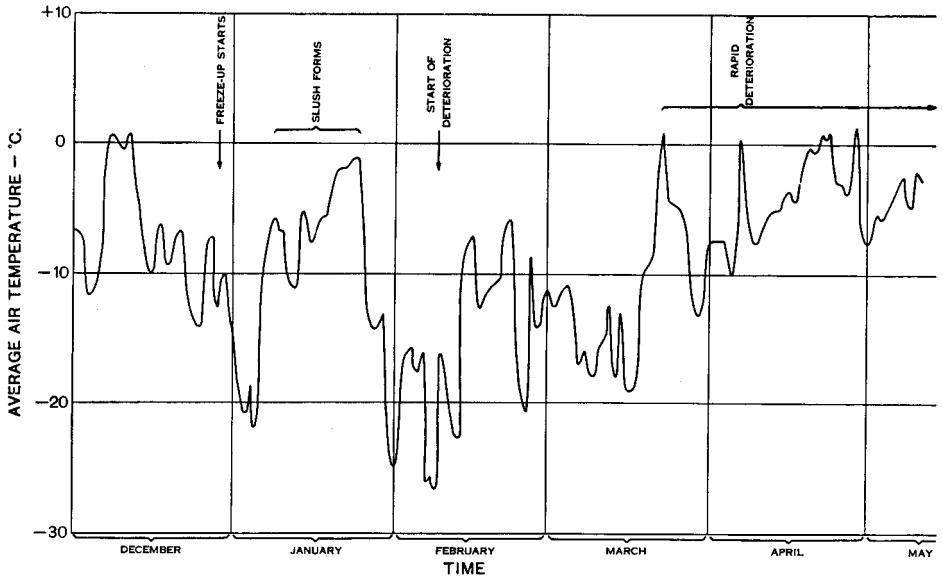
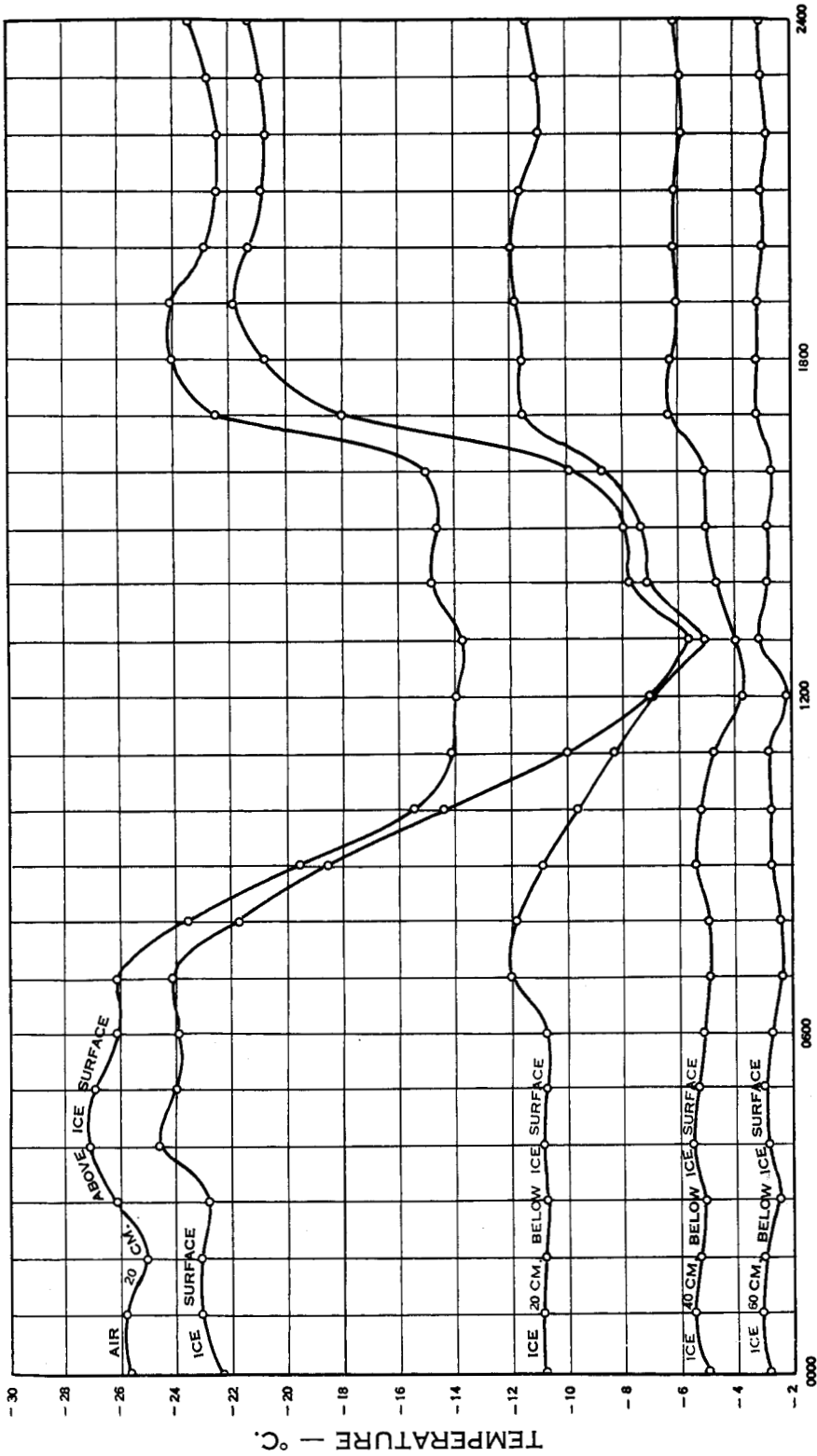


Fig. 11. Graph of daily average air temperatures recorded at the Hopedale Marconi Station from December 1955 to May 1956.

Fig. 12 shows the temperature distribution in the sea-ice cover over a typical 24-hour period (February 25, 1956). Unfortunately, thermocouples were not installed before slush-formation owing to logistic difficulties.

Fig. 13 shows the results of density and thickness profiles of snow and slush made at average intervals of 3 days during the period of slush-formation. The curves show the increase in thickness of the slush layer with time. Fig. 14 presents a comparison of the observed slush-level with the theoretical water-level, which was calculated from the measured density profiles of Fig. 13. At time A (January 6) no snow had fallen and the observed and theoretical water-levels coincided. At time B (January 8) the theoretical water-level was above the surface of the ice but no slush had started to form, whereas at times C and D (January 13 and 17) the calculated water-level was above the observed slush-level. At times E, F, and G, (January 21, 25, and 27) this relation was reversed and the upper surface of the slush-layer was well above the calculated water-level. This information indicates (a) that brine migration through sea-ice was inhibited during the first stages of slush-formation when the ice temperature was lowest and (b) that capillary action was an important factor in determining the upper level of the slush. The density of the 36.8-cm. layer of sea-ice was 0.920 gm./cm.^3 as determined by measuring the height of the ice-surface above the water-level before the snow of January 6. Since the density of the ice would be expected to decrease with time (Fig. 21), the relative importance of capillary action would be increased.



LOCAL STANDARD TIME — FEBRUARY 25, 1956
 Fig. 12. Hourly averages of air and ice temperatures at various levels, local standard time, February 25, 1956.

PHYSICAL PROPERTIES OF SEA-ICE

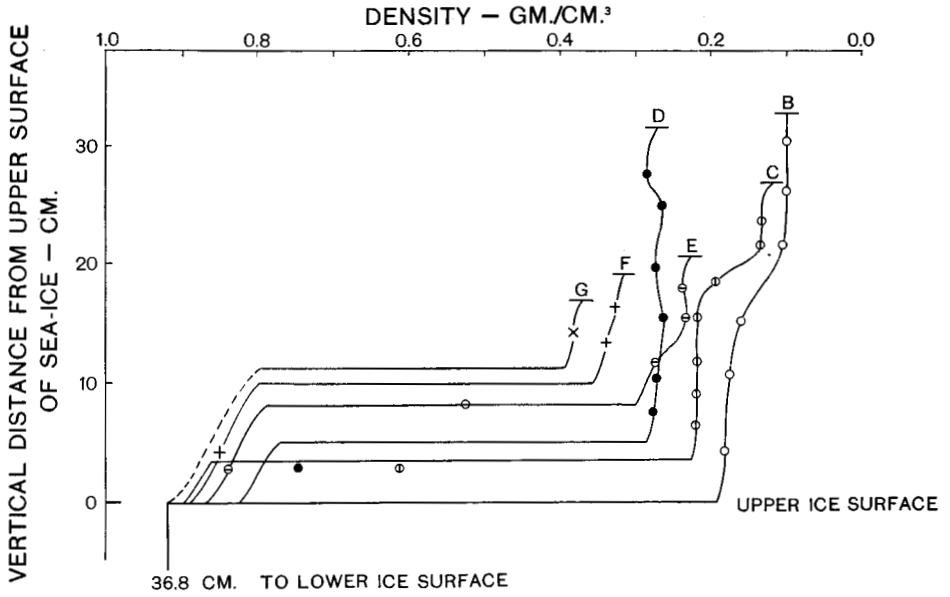


Fig. 13. Graph of snow and slush density and thickness profiles. Dates of profiles are: B January 8, C January 13, D January 17, E January 21, F January 25, and G January 27, 1956.

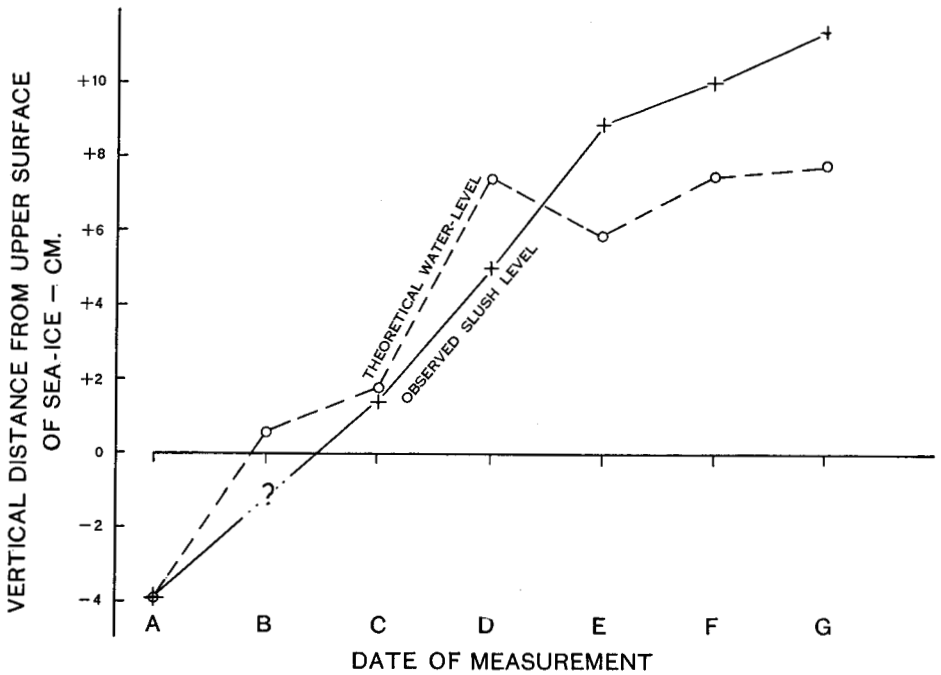


Fig. 14. Observed slush-levels and theoretical water-levels calculated from the data of Fig. 13. Dates of measurements are the same as Fig. 13, except A January 6, 1956.

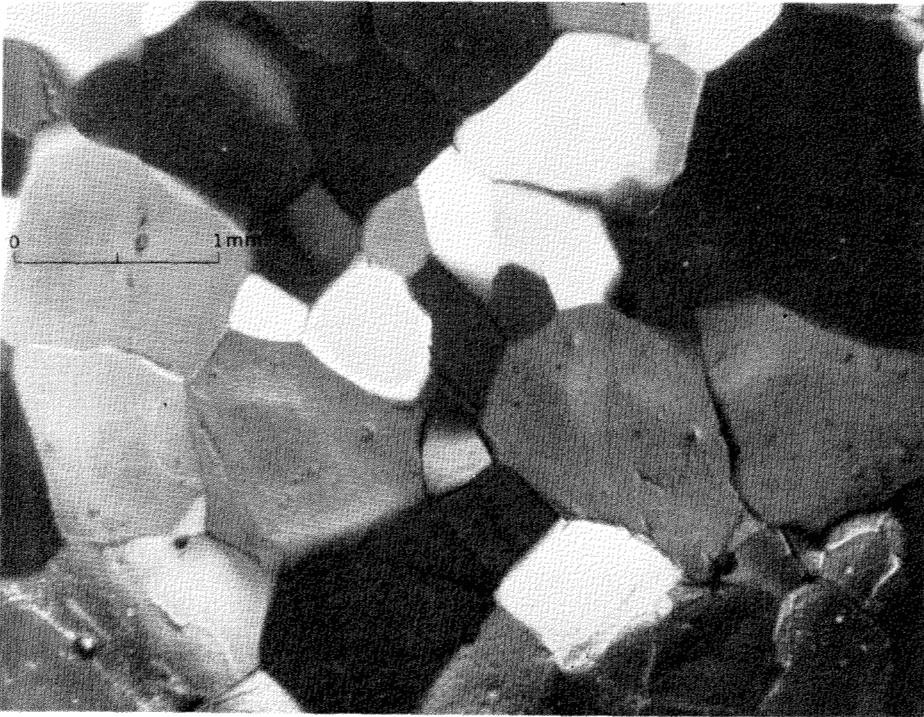


Fig. 15. Photomicrograph of thin section of infiltrated snow-ice.

When the air temperature dropped rapidly on January 25 the slush layer froze into infiltrated snow-ice. This ice layer was in general equigranular, with an average grain size of 1 mm. (Fig. 15) and had a much higher air content and therefore a lower density (approximately 0.83 gm./cm.^3) than normal sea-ice. A Schmidt equal-area net diagram of the c-axis orientation in infiltrated snow-ice shows a strong concentration in the vertical direction (Fig. 16). This orientation may be caused by the formation of ice overgrowths in the same orientation as the snow crystals already present.

When the slush layer froze, it had a high salt content and created an unstable situation in the ice-sheet (a layer of extremely high salinity above a less saline layer); a condition that will tend to stabilize itself at ice temperatures above the critical temperature. Curve k (Fig. 17) shows the salt content of the ice-sheet just before the period of slush-formation. This is a normal vertical distribution of salinity without irregularities. Curve l gives the salinity profile just after the slush layer froze. Note the high salinity of the slush-ice. Curves m and n show the tendency for the denser brine in the upper layers to migrate downward with time. Fig. 18 gives three salinity profiles taken during the deterioration period. They show a uniformly low salinity. The topmost few centimetres of ice (above the water-level) are almost completely free of brine.

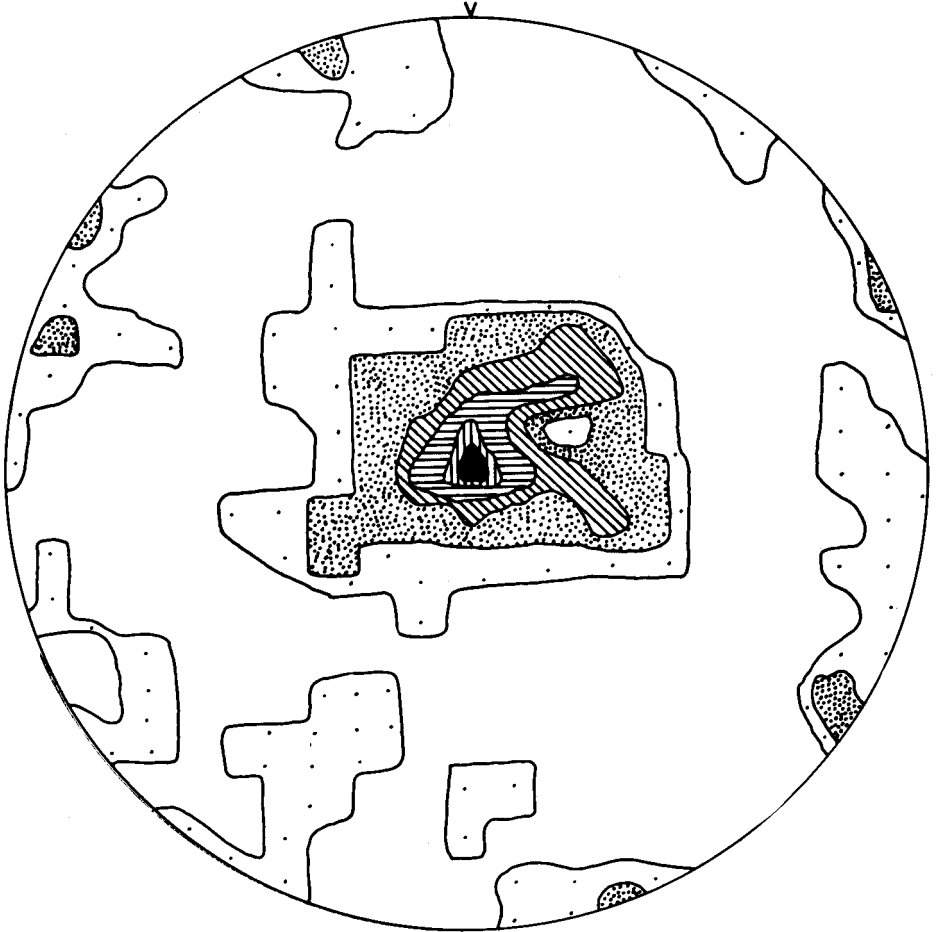


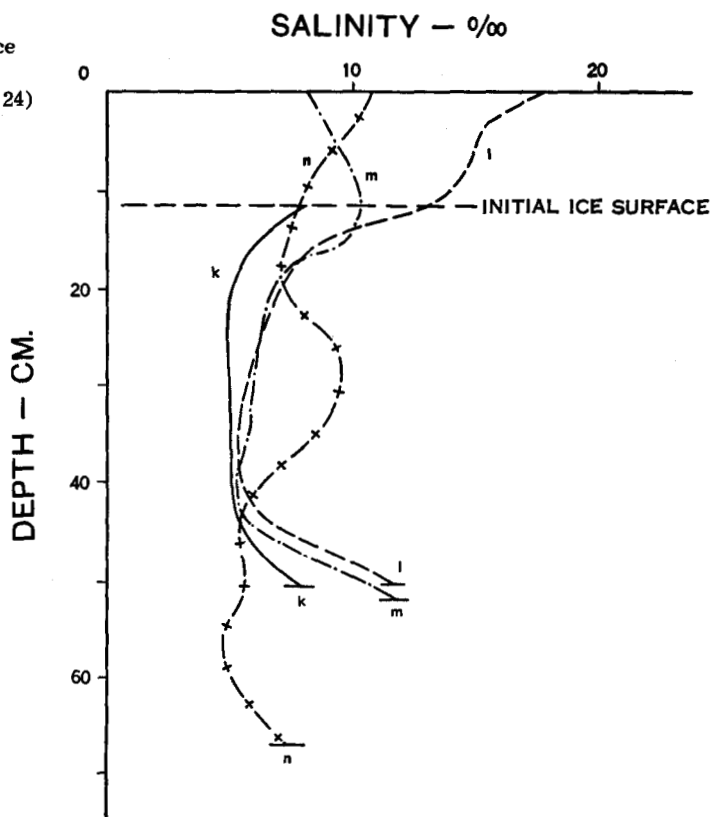
Fig. 16. Orientation of infiltrated snow-ice c-axes plotted on the upper hemisphere of a Schmidt net. Diagram is in the horizontal plane, 200 grains, contours represent 1, 2, 4, 6, 10, and 12 per cent per 1 per cent area.

Fig. 19 shows the average salinity of the ice-sheet plotted against the date of measurement and the thickness of the sheet. The dotted discontinuity in the salt content is due to the freezing of the slush layer. Since the slush layer has an extremely high salt content and the salinity of the pre-existing ice-sheet does not change appreciably during the period of slush-formation, the average salinity of the ice-sheet increases.

Accumulation of sea-ice

To forecast the growth of sea-ice it is usual to employ empirically determined curves that show the relation between observed ice-thickness and accumulated degree-days of frost. Curve A (Fig. 20) is based on ice-

Fig. 17. Salinity profiles from sea-ice taken both before (curve k, January 24) and after the slush-layer froze (curves l, January 27, m, January 30, and n, February 16, 1956).



thickness data collected near the Hopedale dock and refers to a freezing point of -1.8°C . (the freezing point of sea water with a salinity of 32.8‰). Curve B is the empirical equation of Karelin [$N = 2.5 (\Sigma t)^{0.52}$, where N is the ice-thickness in centimetres and Σt is the sum of the mean diurnal negative air temperature]. Karelin's equation represents the maximum sea-ice growth-rate reported in the Russian literature summarized by Lebedev (1940). The Hopedale ice-thickness data for the first 200 degree-days give a smooth, continuous curve and are in good agreement with Karelin's curve. After the period of slush-formation between 210 and 260 degree-days a scatter developed in the measured ice-thickness. This scatter was caused by the uneven distribution of wind-blown snow over the surface of the sea-ice. The heavier the weight of the overlying snow, the more the surface of the sea-ice was depressed below the water-surface, resulting in a correspondingly thicker slush layer. Consequently, after the slush layer froze, the thickest ice was located under the deepest snow-drifts.

The magnitude of this effect is evident from comparing ice-thickness surveys made on January 5, when the maximum variation in thickness owing to dates of initial freezing occurred, with surveys made on January 30 after the first period of slush-formation. The survey of January 5 showed a gradual decrease in ice-thickness from near the dock to Little Snow Island, with the minimum thickness occurring in a late-frozen lead. Ten

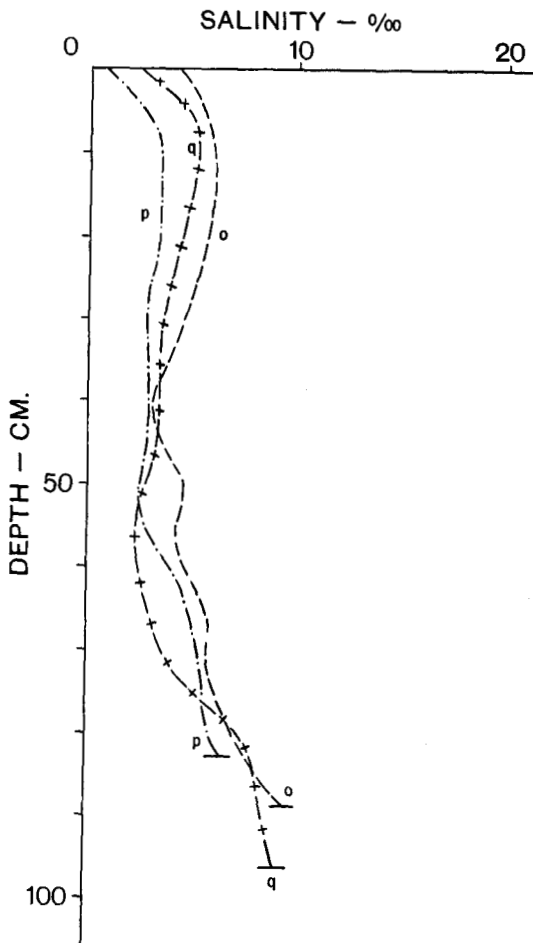


Fig. 18. Salinity profiles from deteriorating sea-ice. Dates of profiles are: o, March 16, p, April 4, and q, May 3, 1956.

measurements gave an average ice-thickness of 29.5 cm. and a standard deviation of 2.2 cm. Any normal ice-growth that took place between the time of these measurements and the slush period would tend to even out these differences because the thinner ice grows faster.

After the period of slush the ice-thickness along this same line averaged 49.1 cm. with a standard deviation of 9.3 cm. At the same time in the lee of the dock, where an extremely large snow-drift had accumulated, an ice-thickness of 95 cm. was measured.

The sudden and sharp increase in ice-thickness for a short period of time at the termination of slush-formation (see Fig. 20) occurred because the slush layer quickly solidified when the air temperature dropped. The slush froze rapidly because it lacked the protection of an insulating thick snow- and ice-layer. Therefore, this portion of the growth curve is similar to the first part of the growth curve that represents the initial freezing of the water body. After the slush layer has frozen the growth curve again parallels the original curve, although slightly offset since the accretion then takes place on the bottom of the ice-sheet. However, the thermal con-

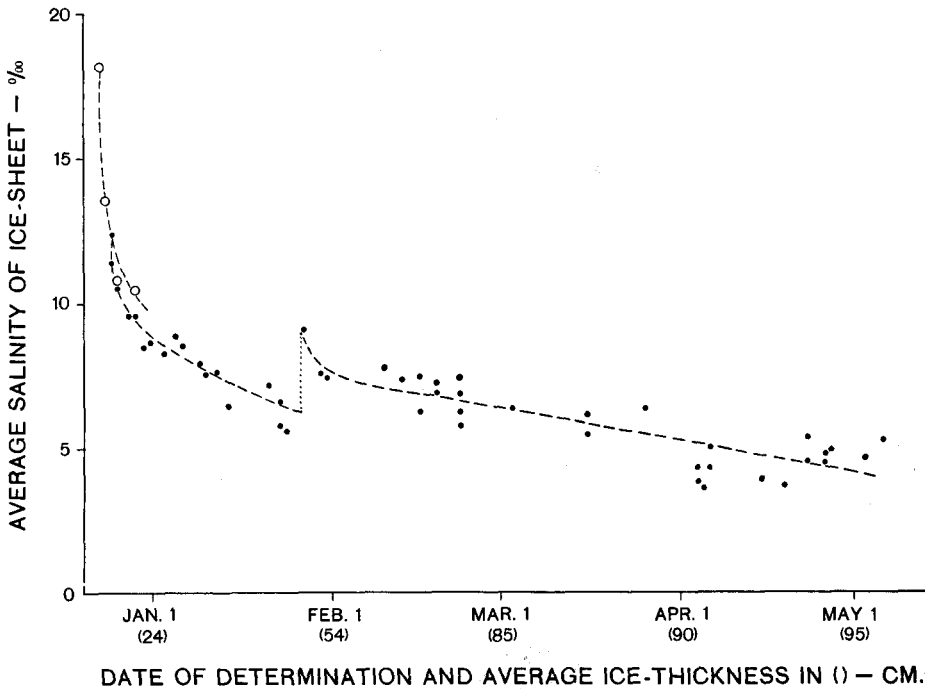


Fig. 19. Average salinity of the ice-sheet plotted against ice-thickness and data of measurement.

ductivity of slush-ice was between 10 and 75 times that of the snow, which it replaced (Mantis, 1950), so that ice accumulation on the lower surface of the slush-ice and sea-ice combination was appreciably greater than it would have been under the initial combination of snow and sea-ice. After the period of slush-formation at Hopedale the measured ice-thickness was *ca.* 20 per cent greater than that given by extrapolation of the initial growth curve.

The observations at Hopedale show that one important assumption that is usually made when computing the ice-thickness can be invalid under subarctic conditions. This is the assumption that in two similar areas that are subject to the same air temperature regime the ice-thickness will vary in inverse relation to the thickness of the snow-cover. In truly arctic regions the formation of infiltrated snow-ice does not take place to any great extent and there the assumption would be valid (Holtsmark, 1955).

Density of sea-ice

Sea-ice densities measured at Hopedale were determined in the following manner: a 7.6-cm.-diameter vertical core was taken from the ice-sheet. The core was cut into segments of approximately 7.6-cm. length. Each

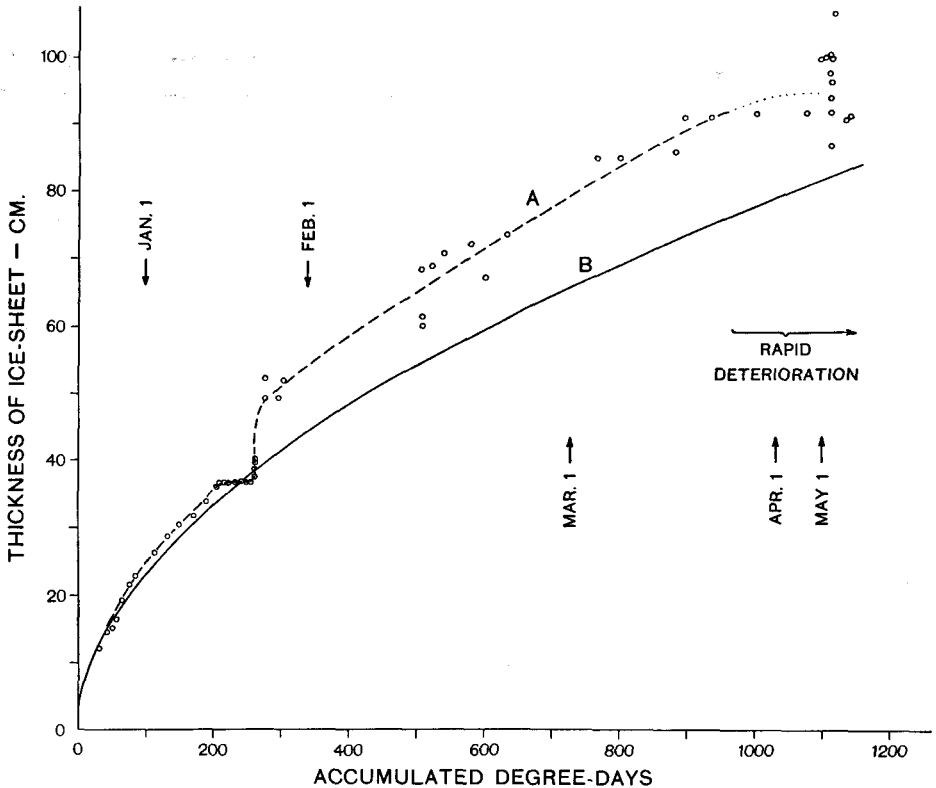


Fig. 20. Comparison of Hopedale (A) and Russian (B) degree-day curves. The sources of the curves are described in the text.

segment was measured accurately and its volume was computed. The density of each sample was determined after the cylinder was weighed. Salinities were determined from the melt water of the ice samples.

Fig. 21 shows sea-ice densities from four different periods plotted against their median locations in the ice-sheet. From examination of these data the following conclusions are drawn:

1. The density of the infiltrated snow-ice is in general lower than that of normal sea-ice.
2. There does not appear to be a systematic variation in density with depth of the sample in the ice-sheet.
3. In general the average density of the ice-sheet decreases with the age of the sheet [period 1, $\rho = 0.920$; period 2, $\rho = 0.904$; period 3, $\rho = 0.880$]. Unfortunately, densities of newly formed sea-ice at Hopedale were not determined. However, measurements at Thule, Greenland the following winter showed that the average density of newly formed sea-ice was *ca.* 0.945 gm./cm.^3 . This density decrease with time is quite understandable since during the aging

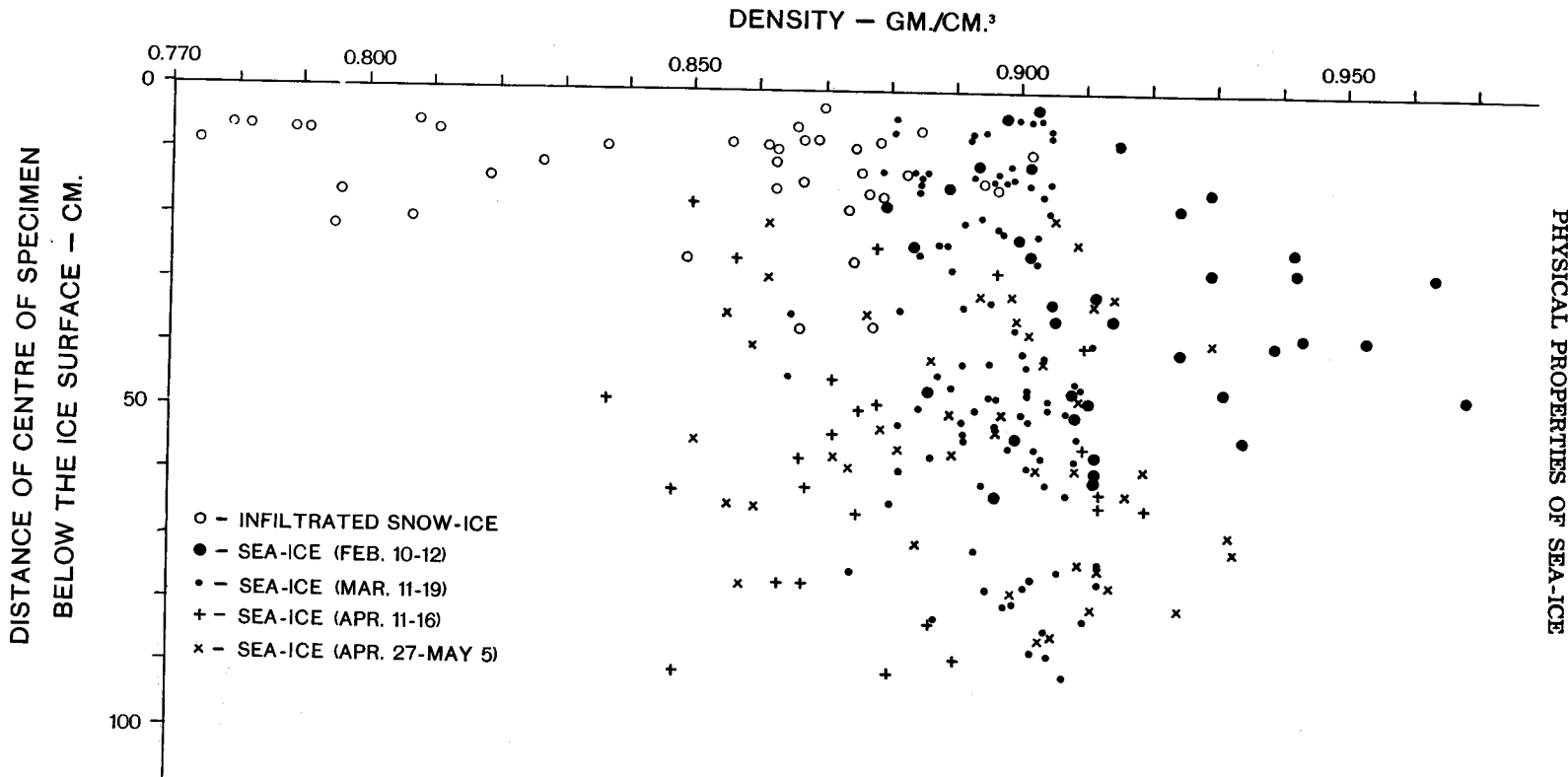


Fig. 21. Density measurements of sea-ice at Hopedale.

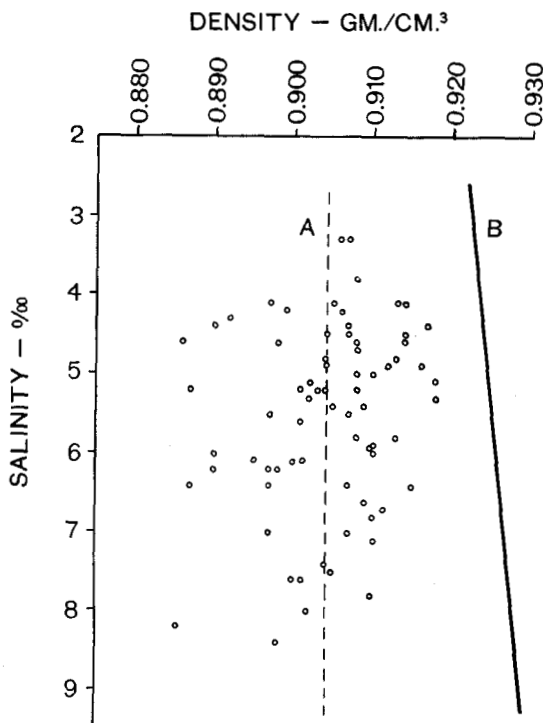


Fig. 22. Comparison of ice-densities measured during the period of March 11 to 19, 1956, with the theoretical density of air-free sea-ice at -15°C . (line B).

process part of the brine cells are replaced by ice. The ice of period 4, however, has an average density of 0.902 gm./cm.^3 .

Fig. 22 presents sea-ice densities measured between March 11 to 19 plotted as a function of salinity. Line A is a least-squares fit of the data. Line B (Zubov, 1945) shows the theoretical density of air-free sea-ice at -15°C . (the average air temperature during this period of time). Comparing these two curves it can be seen that since the sea-ice of this period has an average density of 0.904 gm./cm.^3 instead of 0.926 gm./cm.^3 it contains 2.4 per cent by volume of air.

Crack-formation

Observations were made on the distribution and history of tidal and thermal cracks in Hopedale Bay. Fig. 1 shows the location of the major zones of thermal contraction cracks in the ice-sheet. The following conclusions are drawn:

1. Thermal cracks usually form between headlands (points) or other topographic irregularities. These cracks form in the same locations year after year.
2. The ice-crystals found in narrow, healed cracks have their c-axes horizontal and in line with the crack.

3. Healed cracks appear to be stronger than the normal ice-sheet. Once a crack has been frozen it usually does not break open again; but similar cracks will form parallel to it.
4. Cracks caused by tidal motion are localized near shore.

Acknowledgements

The field observations on which this paper is based were made while the authors were associated with the Geophysics Research Directorate, Air Force Cambridge Research Center (W.F.W.) and the U.S. Navy Hydrographic Office, Applied Oceanography Branch, Washington 25, D.C. (O.S.L.). One of the authors (W.F.W.) would also like to acknowledge the sponsorship of the Geophysics Research Directorate of the Air Force Cambridge Research Center, Air Research and Development Command, under Contract No. AF 19 (604)-3062. The density determinations presented in Fig. 21 were taken by P. Pomroy (February 10 to 12), T. R. Butkovich (March 11 to 19), N. Costes (April 11 to 16), and Dr. A. Assur (April 27 to May 5). We are also indebted to them for many profitable discussions in the field. Thanks are also due to W. H. Hymes who assisted in the field observations. More detailed analyses of specific problem areas investigated during this project that have been published or that are now in press are: Anderson and Weeks (1958), Butkovich (1956), Weeks (1958), Weeks and Anderson (1958 a, b).

References

- Anderson, D. L. and W. F. Weeks. 1958. A theoretical analysis of sea-ice strength. *Trans. Am. Geophys. Union* 39:632-40.
- Armstrong, T. 1954. Sea ice studies. *Arctic* 7:201-5.
- Bader, H. 1957. Ice drills and corers. *J. Glac.* 3:30.
- Butkovich, T. R. 1956. Strength studies of sea-ice. SIPRE Research Report No. 20, 15 pp.
- Holtsmark, B. E. 1955. Insulating effect of a snow cover on the growth of young sea ice. *Arctic* 8:60-65.
- Lebedev, V. V. 1940. New formulas on the growth of ice in arctic rivers and seas. *Meteorologiya i Gidrologiya* 6:40-51.
- Mantis, H. T. *et al.* 1951. Review of the properties of snow and ice. SIPRE Report No. 4, 156 pp.
- Weeks, W. F. 1958. The structure of sea ice. A progress report. NAS Sea Ice Conference Proceedings.
- Weeks, W. F. and D. L. Anderson. 1958a. Sea ice thrust structures. *J. Glac.* 3:173-5.
- _____ 1958b. An experimental study of the strength of young sea ice. *Trans. Am. Geophys. Union* 39:641-7.
- Weeks, W. F. and O. S. Lee. 1957. Observations on the growth of sea ice at Hopedale, Labrador. (Abstr.) *Trans. Am. Geophys. Union* 38:412.
- Wilson, J. T., J. H. Zumberge, and E. W. Marshall. 1954. A study of ice on an inland lake. SIPRE Research Report No. 5, 78 pp.
- Zubov, N. N. 1945. *Ledy arktiki (Ice of the Arctic)*. Moscow: Izdatelestvo Glavsevmorputi, 360 pp.